Geophysical Prospecting, 1996 44, 3–26

Plane-layered models for the analysis of wave propagation in reservoir environments[1]

José M. Carcione[2]

Abstract

The long-wavelength propagation and attenuation characteristics of three geological structures that frequently occur in reservoir environments are investigated using a theoretical model that consists of a stack of fine and viscoelastic plane layers, with the layers being either solid or fluid. Backus theory properly describes fine layering and a set of fluid-filled microfractures, under the assumption that interfaces between different materials are bonded. The effects of saturation on wave attenuation are modelled by the relative values of the bulk and shear quality factors.

The anisotropic quality factor in a fine-layered system shows a variety of behaviours depending on the saturation and velocities of the single constituents. The wave is less attenuated along the layering direction when the quality factors are proportional to velocity, and vice versa when inversely proportional to velocity. Fractured rocks have very anisotropic wavefronts and quality factors, in particular for the shear modes which are strongly dependent on the characteristics of the fluid filling the microfractures.

When the size of the boundary layer is much smaller than the thickness of the fluid layer, the stack of solid–fluid layers becomes a layered porous media of the Biot type. This behaviour is caused by the slip-wall condition at the interface between the solid and the fluid. As in Biot theory, there are two compressional waves, but here the medium is anisotropic and the slow wave does not propagate perpendicular to the layers. Moreover, this wave shows pronounced cusps along the layering direction, like shear waves in a very anisotropic single-phase medium.

Introduction

A stack of plane and parallel layers is a useful model for studying the wave propagation characteristics of basic geological and rock structures. In particular, the systems investigated in this work are predominant in reservoir environments at

[1] Paper presented at the 54th EAEG meeting, Paris, June 1992. Received October 1992, revision accepted April 1995.

[2] Osservatorio Geofisico Sperimentale, PO Box 2011, Opicina, I-3401 Trieste, Italy.

different spatial scales. The theory may also be applied to the analysis of laminated composite media and certain geological structures that contribute to the formation of sedimentary basins.

In a previous paper (Carcione 1992), the model was used to study the anisotropic characteristics of attenuation for waves propagating in a viscoelastic finely layered medium composed of two constituents. It is well known (Postma 1955) that when the thicknesses of the component layers are much smaller than the wavelength of the seismic pulse, a stratified medium can be replaced by an equivalent homogeneous transversely isotropic medium. For a viscoelastic system, the complex stiffness matrix is given by Backus equations through application of the correspondence principle. Carcione (1992) calculated the energy velocities and quality factors of the three propagating modes as a function of frequency and material proportions. He obtained in this way a model for describing anisotropic attenuation in fine layering due to intrinsic loss mechanisms.

In this work, three realistic models built with a stack of viscoelastic plane solid and/or fluid layers are investigated. Wave attenuation is described by a continuous relaxation model, giving an almost constant quality factor over a broad frequency band. Firstly, attenuation in fine layering is analysed for cases where the quality factor Q is proportional to wave velocity, and then when Q is proportional to the inverse of the wave velocity. Rocks show different attenuation depending on whether they are dry, saturated or partially saturated. In the first two cases, the quality factor of compressional waves is higher than the quality factor of shear waves; the opposite occurs when rocks are partially saturated. These situations are also investigated and, additionally, the characteristics of systems with more than two constituents are analysed.

A stack of two-constituent plane layers is used to describe a system of long and thin fluid-filled microfractures and cracks. This is an appropriate model because cracks are likely to be preferentially aligned by a variety of non-lithostatic stress and stress-induced processes. Moreover, such fluid-filled cracks are usually realigned by subcritical crack growth. The fracture-filling material is modelled by a non-Newtonian viscoelastic fluid represented by a 'soft' Kelvin-Voigt constitutive relation whose rigidity is small compared to typical rock rigidities. This model gives a complex viscosity appropriate for modelling the behaviour of fluids with solid inclusions (colloid-type), and fluids in the presence of strong pore surface effects. The model shows how the wave propagation characteristics of fractured formations and rocks depend on the scale and frequency content of the probing pulse. For instance, the results apply to fluid-filled joints and fractured systems of rotational symmetry distributed over large areas, or to wave propagation on a smaller scale, when fluids permeate the cleavage planes of metamorphic and sedimentary rocks. In all the cases, the quality factors due to intrinsic loss mechanisms show anisotropic effects through preferred orientations. A similar model for fractured systems (Schoenberg and Douma 1988) was shown to be effective even for aspect ratios up to 0.3 and crack densities up to 0.03.

The fracture model assumes that the skin depth of the boundary layer is much larger than the thickness of the fluid layers, or equivalently, that the wavelength of the viscous wave is much larger than the thickness of the fracture. When the skin depth is small in comparison with the thickness of the fracture, the model of alternating solid and fluid layers becomes a layered porous medium of the Biot type, where the solid is the matrix and the relative fluid proportion is the porosity (Schoenberg 1984). The model applies when the wavelength is much larger than the thickness of the pore, but much smaller than its length. This situation may occur for high frequencies in fractured limestones, where the aspect ratio of the pores is very low. Thus, the results may give an indication of the wave phenomena taking place at the microstructural level. The dynamic coupling between the solid and the fluid layers varies according to the propagation angle. For propagation perpendicular to the layers, only the fast wave propagates, corresponding to in-phase motion of the system. For angles out of the normal, the slow wave, with the solid and fluid displacements 180° out of phase, starts to develop and reaches its maximum decoupling along the layering direction. The anisotropic and attenuation characteristics of these compressional modes are analysed as a function of the porosity and the dissipation properties of the solid and fluid phases.

Layered media with bonded interfaces

The model representing a stratified medium is made up of homogeneous isotropic plane layers which are perfectly bonded, i.e. there is no interfacial slip. Let there be N different materials, each one occupying the same proportion in a sufficiently large sample of stratified medium.

Let each single isotropic medium be anelastic with complex Lamé parameters given by

$$\lambda = (\lambda^e + \tfrac{2}{3}\mu^e)M_1 - \tfrac{2}{3}\mu^e M_2 \quad \text{and} \quad \mu = \mu^e M_2, \tag{1}$$

where M_1 and M_2 are dimensionless complex moduli in dilatation and shear, respectively, and λ^e and μ^e are the low-frequency limit Lamé constants. The theory assumes constant quality factors over the frequency range of interest. Such behaviour is modelled by a continuous distribution of relaxation mechanisms based on the standard linear solid (Ben-Menahem and Singh 1981). The dilatational and shear dimensionless complex moduli can be expressed as

$$M_\nu(\omega) = \left[1 + \frac{2}{\pi \bar{Q}_\nu} \ln\left(\frac{1 + i\omega\tau_2}{1 + i\omega\tau_1}\right)\right]^{-1}, \qquad \nu = 1, 2, \tag{2}$$

where τ_1 and τ_2 are time constants, with $\tau_2 < \tau_1$, and $\bar{Q}_\nu$ defines the value of the quality factor, which remains nearly constant over the selected frequency range. The low-frequency limit shows elastic behaviour with $M_\nu \to 1$; the high-frequency limit is also elastic with $M_\nu \to 1/[1 + (2\pi/\bar{Q}_\nu) \ln (\tau_2/\tau_1)]$. The bulk and shear quality factors are given by

$$Q_\mathrm{k} = \frac{\mathrm{Re}\,(M_1)}{\mathrm{Im}\,(M_1)} \quad \text{and} \quad Q_\mathrm{S} = \frac{\mathrm{Re}\,(M_2)}{\mathrm{Im}\,(M_2)} \tag{3}$$

respectively, and the quality factor corresponding to the compressional wave is

$$Q_\mathrm{P} = \frac{\mathrm{Re}\,(\lambda + 2\mu)}{\mathrm{Im}\,(\lambda + 2\mu)}. \tag{4}$$

As illustrated in Fig. 1a, for $\lambda_{\min} \gg L$ (see Postma 1955; Carcione, Kosloff and Behle 1991), where $\lambda_{\min}$ is the minimum wavelength, the stratified medium can be replaced by an effective homogeneous transversely isotropic medium whose stiffness components c_{IJ}, $I, J = 1, \ldots, 6$ are frequency-dependent and complex. The dependence of the c_{IJ} on λ and μ can be found in Backus (1962) or in Carcione (1992).

The displacement of a general viscoelastic plane wave is of the form

$$\mathbf{u} = \mathbf{U}_0 \exp\,[\mathrm{i}(\omega t - \mathbf{k}\cdot\mathbf{x})], \tag{5}$$

where t is the time variable, $\mathbf{x}$ is the position vector, and $\mathbf{k}$ is the complex wavenumber vector defined by

$$\mathbf{k} = \boldsymbol{\kappa} - \mathrm{i}\boldsymbol{\alpha}, \tag{6}$$

with $\boldsymbol{\kappa}$ and $\boldsymbol{\alpha}$ being the propagation and attenuation vectors, respectively. When these vectors are colinear, the wave is called homogeneous and the wavevector is given by

$$\mathbf{k} = (\kappa - \mathrm{i}\alpha)\hat{\boldsymbol{\kappa}} \equiv k\hat{\boldsymbol{\kappa}}, \tag{7}$$

where

$$\hat{\boldsymbol{\kappa}} = l_x\hat{\mathbf{e}}_x + l_y\hat{\mathbf{e}}_y + l_z\hat{\mathbf{e}}_z \tag{8}$$

defines the propagation direction through the direction cosines l_x, l_y and l_z.

Since the stratified medium has azimuthal symmetry, it is enough to consider propagation in, say, the (x, z)-plane, for which $l_y = 0$. Then, the complex Christoffel equation (e.g. Auld 1990) reads

$$\begin{bmatrix} c_{11}l_x^2 + c_{55}l_z^2 & 0 & (c_{13}+c_{55})l_xl_z \\ 0 & c_{66}l_x^2 + c_{55}l_z^2 & 0 \\ (c_{13}+c_{55})l_xl_z & 0 & c_{55}l_x^2 + c_{33}l_z^2 \end{bmatrix} \mathbf{u} = \rho V^2\mathbf{u}, \tag{9}$$

where V is the complex velocity. Equation (9) gives a complex dispersion equation with three solutions, two coupled modes denoted by qP and qSV, representing the quasi-compressional and quasi-shear waves, and a pure shear (SH) mode, whose displacement vector is parallel to the layering. Expressions for the complex, phase and energy velocities, attenuation factor, quality factor and slowness vector, in

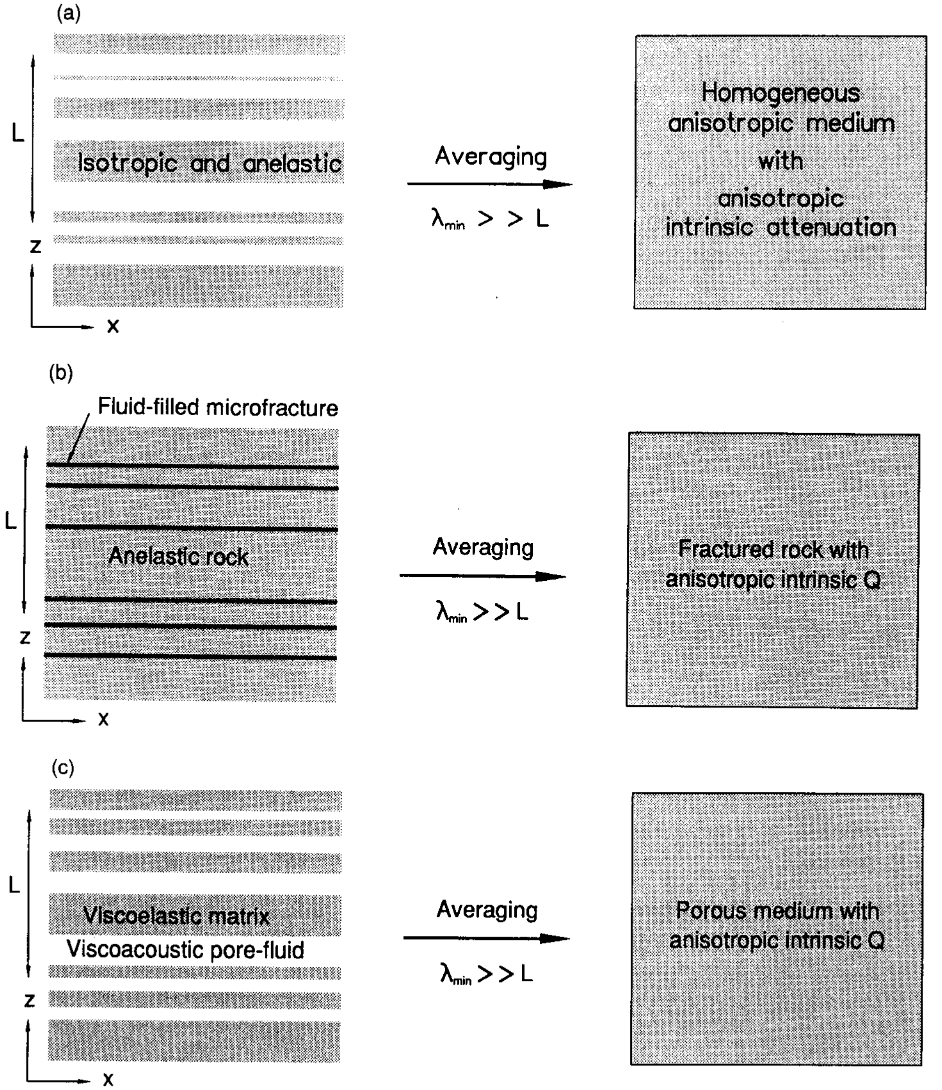

Figure 1. (a) A stratified medium whose constituents are anelastic can be replaced by a homogeneous medium with anisotropic wave attenuation when the minimum wavelength λ_{min} is much larger than a sufficiently large sample of length L. (b) Backus theory can be used to describe a system of fluid-filled long and planar microfractures provided that the size of the fluid boundary layer is greater than the thickness of the fracture. Moreover, if the fluid and the matrix rock are dissipative, the averaged system possesses an anisotropic intrinsic Q. (c) A model for layered porous media is obtained with alternating solid and fluid layers, the solid representing the matrix and the fluid proportion, the porosity. At the long-wavelength limit, this model is a Biot anisotropic medium when the thickness of the fluid layers is large in comparison with the viscous wavelength. In this case, the fluid can be considered practically ideal, and perfect interfacial slip takes place.

terms of the complex stiffnesses c_{IJ} and propagation direction $\hat{\kappa}$, are given by Carcione (1992). Since the equivalent medium is anelastic, the energy velocity (not the group velocity) is used to define the wavefront (see Carcione 1994).

Viscoelasticity finely layered media

The first example presents a stationary medium composed of limestone and sandstone whose elastic properties, including density and wave velocities, are given in Table 1. Let the time constants in (2) be $\tau_1 = 0.16$ s and $\tau_2 = 3 \times 10^{-4}$ s, so that the quality factors are nearly constant over a broad frequency range including the exploration seismic band. Figure 2 shows zonal sections of the slownesses, energy velocities and quality factors of the three wave modes in the equivalent medium, at a frequency of 25 Hz. The quality factors for the limestone are $\bar{Q}_1 = 80$ and $\bar{Q}_2 = 40$, and for the sandstone, $\bar{Q}_1 = 60$ and $\bar{Q}_2 = 20$, corresponding to fully saturated

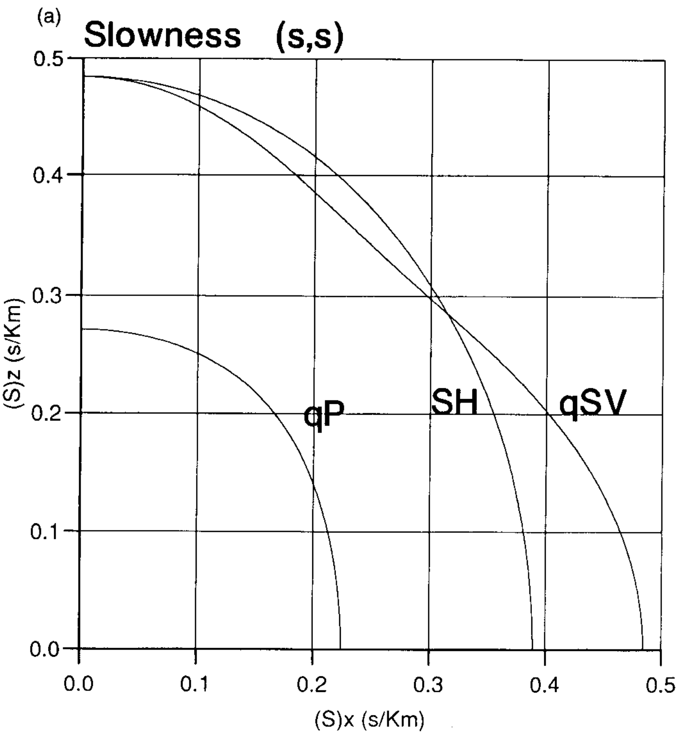

Figure 2. Zonal sections of (a) the slowness, (b) energy velocity and (c) quality factor surfaces for a fully saturated stratified medium. The medium is composed of limestone and sandstone with quality factors $\bar{Q}_1 = 80$ and $\bar{Q}_2 = 40$, and $\bar{Q}_1 = 60$ and $\bar{Q}_2 = 20$, respectively. The symbol (s, s) indicates that both constituents (limestone and sandstone) are fully saturated.

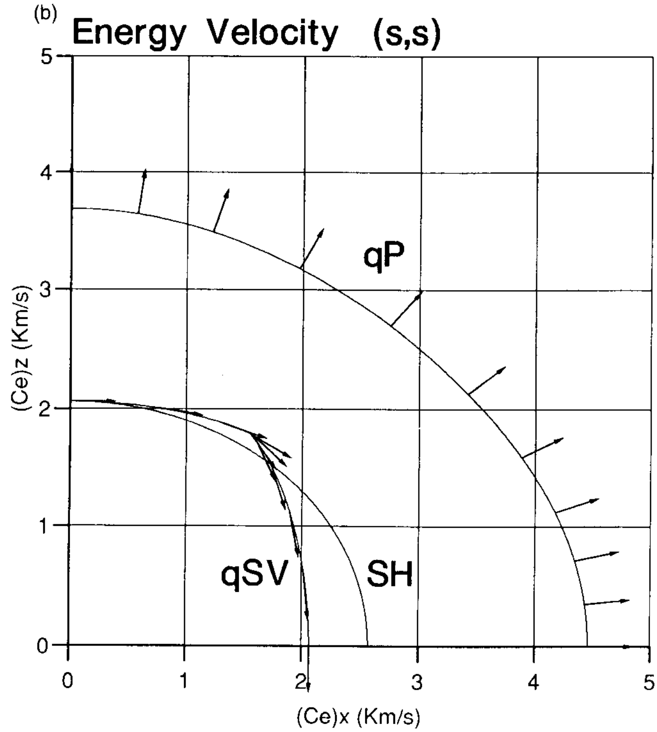

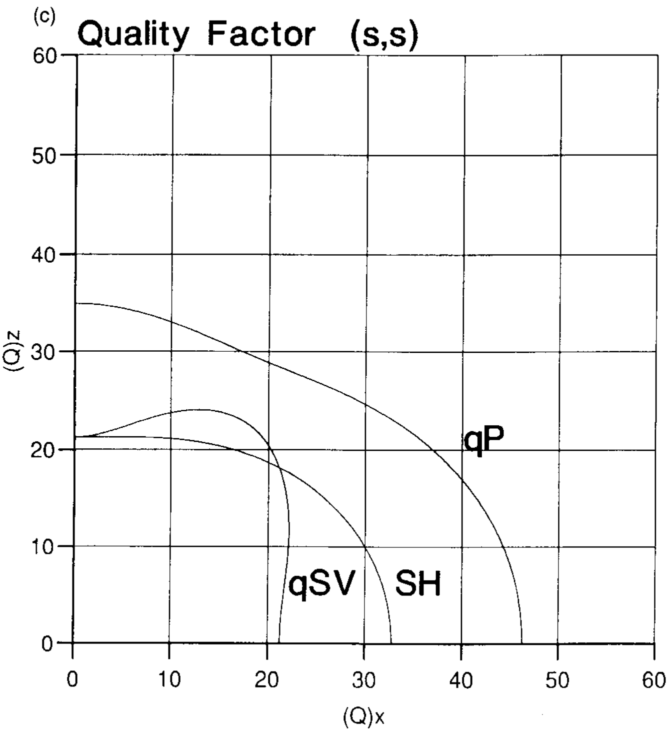

Figure 2. Continued

Table 1. Material Properties

Medium	λ^e (GPa)	μ^e (GPa)	ρ (Kg/m^3)	c_P (m/s)	c_S (m/s)
limestone	30	25	2700	5443	3043
sandstone	8	6	2300	2949	1615
shale	6.28	1.70	2250	2074	869

rocks. The symbol (s, s) in Fig. 2 indicates that both constituents (limestone and sandstone, respectively) are fully saturated, such that

$$(\mathrm{s},\ \mathrm{s}) \equiv [(\bar{Q}_1,\ \bar{Q}_2)_{\mathbf{limestone}},\ (\bar{Q}_1,\ \bar{Q}_2)_{\mathbf{sandstone}}] = [(80,\ 40),\ (60,\ 20)]$$

in terms of the quality factors. The polarizations are plotted on the energy velocity curves; when not plotted, they are normal to the plane of the figure (the polarization vectors for anisotropic-viscoelastic media are calculated in Appendix A). The deviation of the viscoelastic polarization from the elastic polarization is shown in Fig. 3 where $\Delta\gamma$ is the difference between the polarization angles with respect to the x-axis.

Figure 4 shows the results of all possible combinations of the quality factors; for instance, both rocks being partially saturated means that (ps, ps) $\equiv$ [(40, 80), (20, 60)], and attenuation being inversely proportional to the velocity means that (s, s)i $\equiv$ [(60, 20), (80, 40)]. An example in which only one of the constituents is saturated is given by (s, ps)i $\equiv$ [(60, 20), (40, 80)]. In general, attenuation is higher along the symmetry axis when the quality factors are proportional to the wave

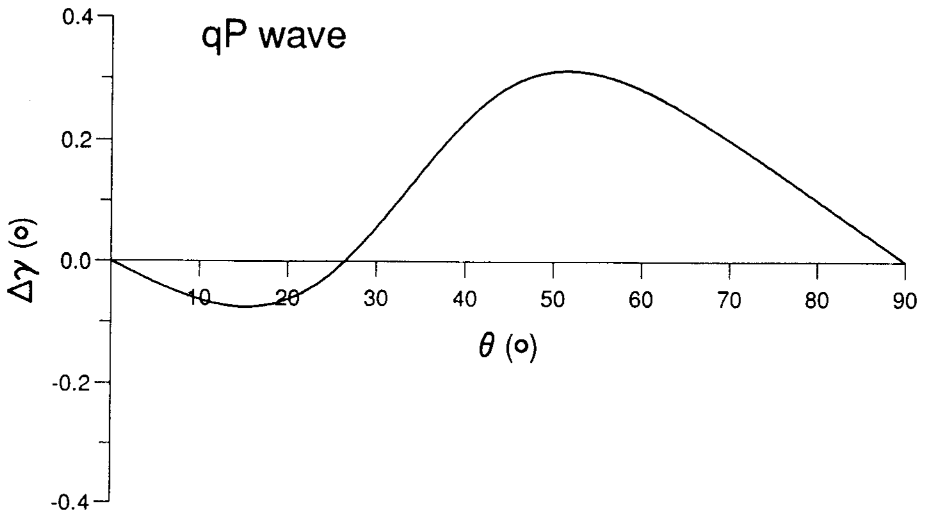

Figure 3. Deviation of the viscoelastic polarization from the elastic polarization for the qP wave. The angles are measured with respect to the x-axis.

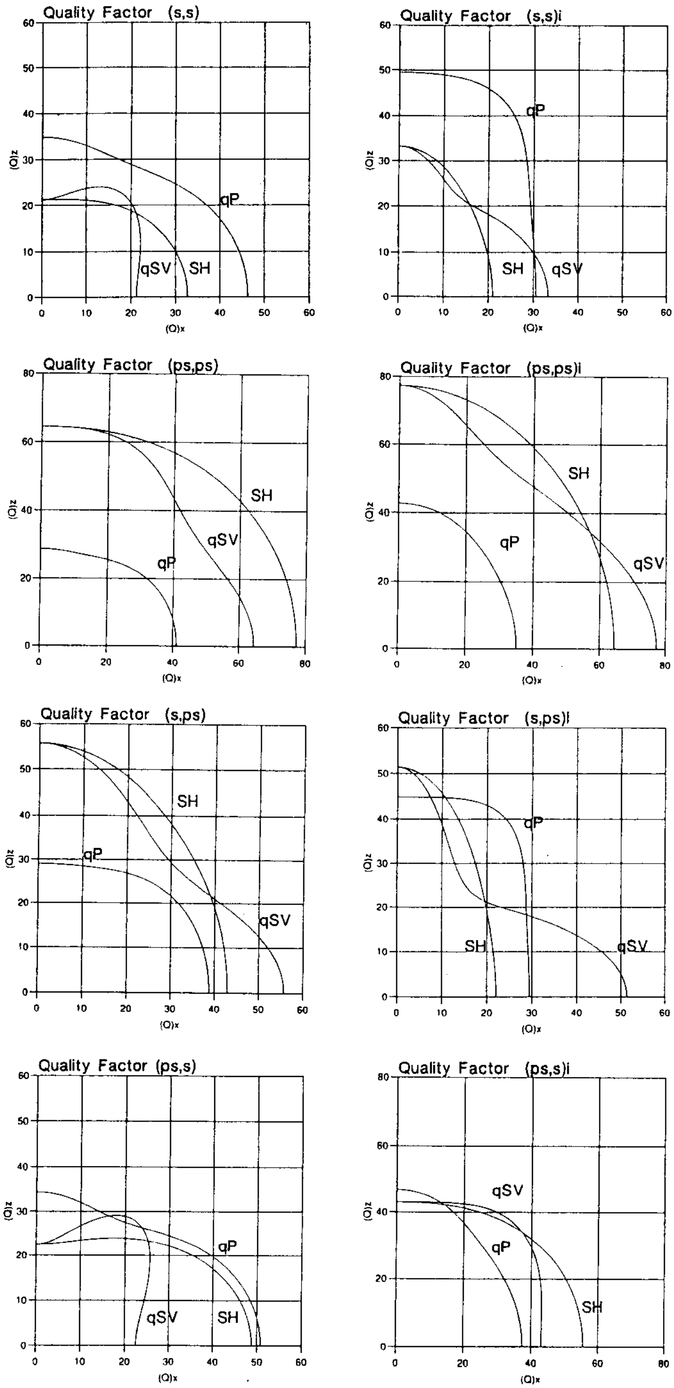

Figure 4. All possible quality factors for the limestone–sandstone system. Both constituents being fully saturated is represented by (s, s) ≡ [(80, 40), (60, 20)] in terms of the quality factors; partial saturation is represented by (ps, ps) ≡ [(40, 80), (20, 60)]; attenuation inversely proportional to the velocity is represented by (s, s)i ≡ [(60, 20), (80, 40)]; and only one of the constituents being saturated is represented by (s, ps)i ≡ [(60, 20), (40, 80)].

velocity, and vice versa when the quality factors are inversely proportional to the velocity. The coupled qSV shear mode has similar attenuation at the horizontal and vertical axes but is very anisotropic at intermediate directions.

The following example considers an equivalent transversely isotropic medium composed of ten isotropic constituents whose material properties are obtained from the intermediate linear interpolated values of the limestone and shale rocks given in Table 1. The bulk quality factor varies from $\bar{Q}_1 = 80$ (limestone) to $\bar{Q}_1 = 20$ (shale), and the shear quality factor from $\bar{Q}_2 = 60$ to $\bar{Q}_2 = 10$, when the system is fully saturated. Its physical properties are shown in Fig. 5. Compared to the limestone–sandstone, this system is more anisotropic (in particular the quality factors). Figure 6 shows the quality factors for the partially saturated medium (a), and for homogeneous $\bar{Q}_2 = 50$ (b). In this case, the uncoupled shear (SH) mode has isotropic attenuation, but the qSV mode is anisotropic due to the coupling with the compressional wave.

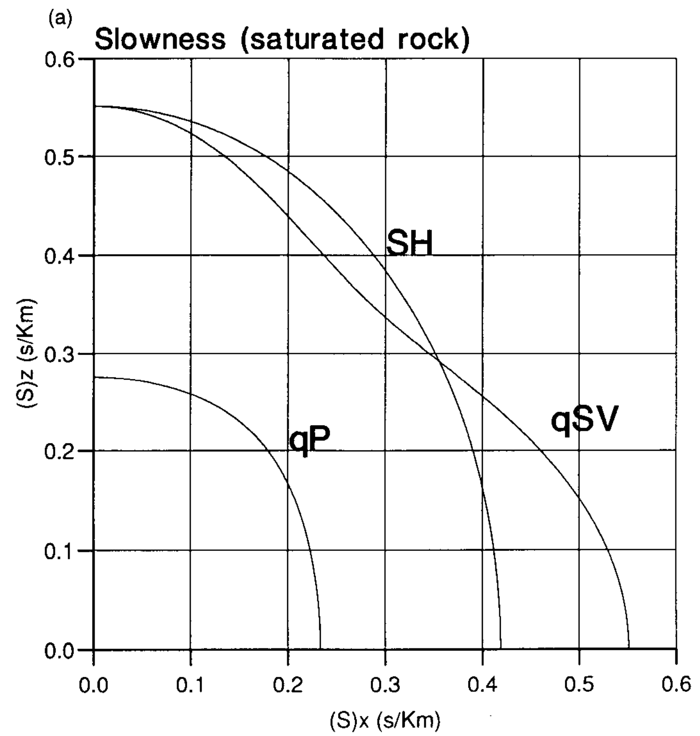

Figure 5. Zonal sections of (a) the slowness, (b) energy velocity and (c) quality factor surfaces for a fully saturated stratified medium composed of ten constituents whose material properties are obtained from the shale and limestone rocks given in Table 1. The bulk quality factor varies from $\bar{Q}_1 = 80$ (limestone) to $\bar{Q}_1 = 20$ (shale), and the shear quality factor from $\bar{Q}_2 = 60$ to $\bar{Q}_2 = 10$.

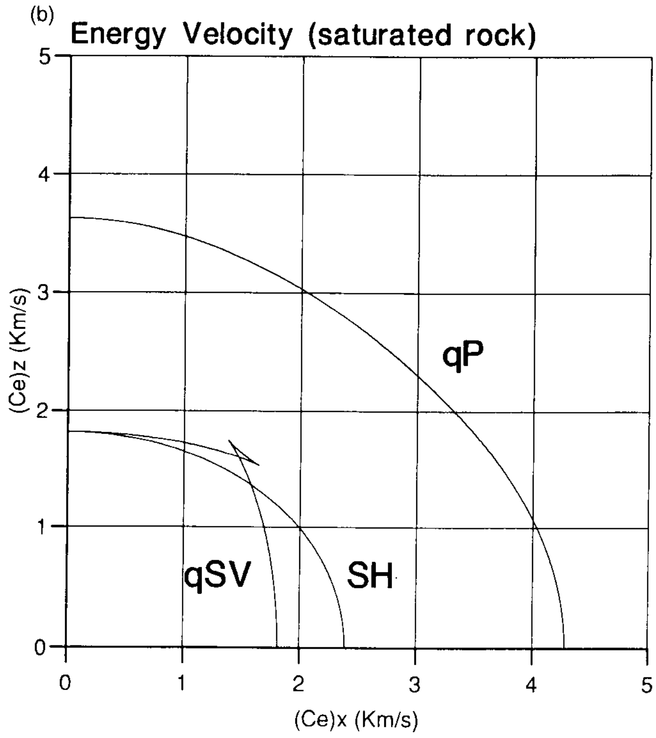

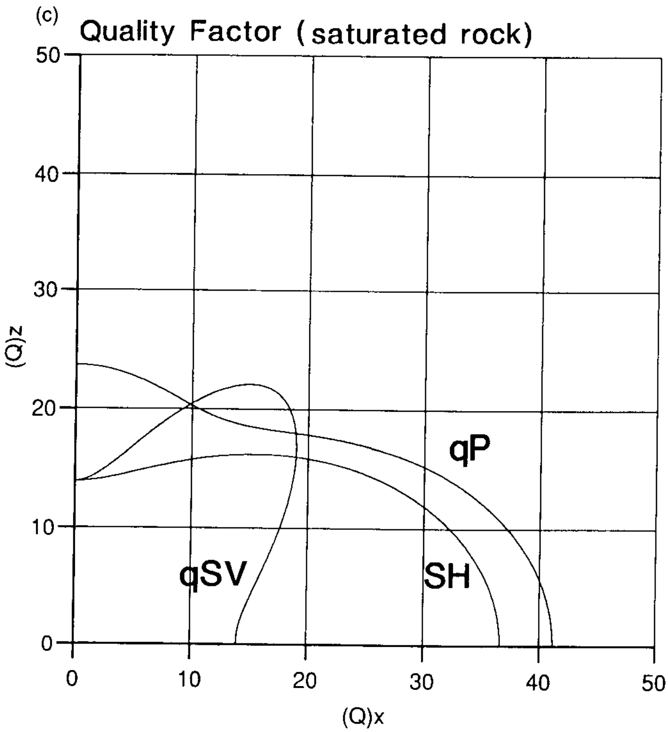

Figure 5. Continued

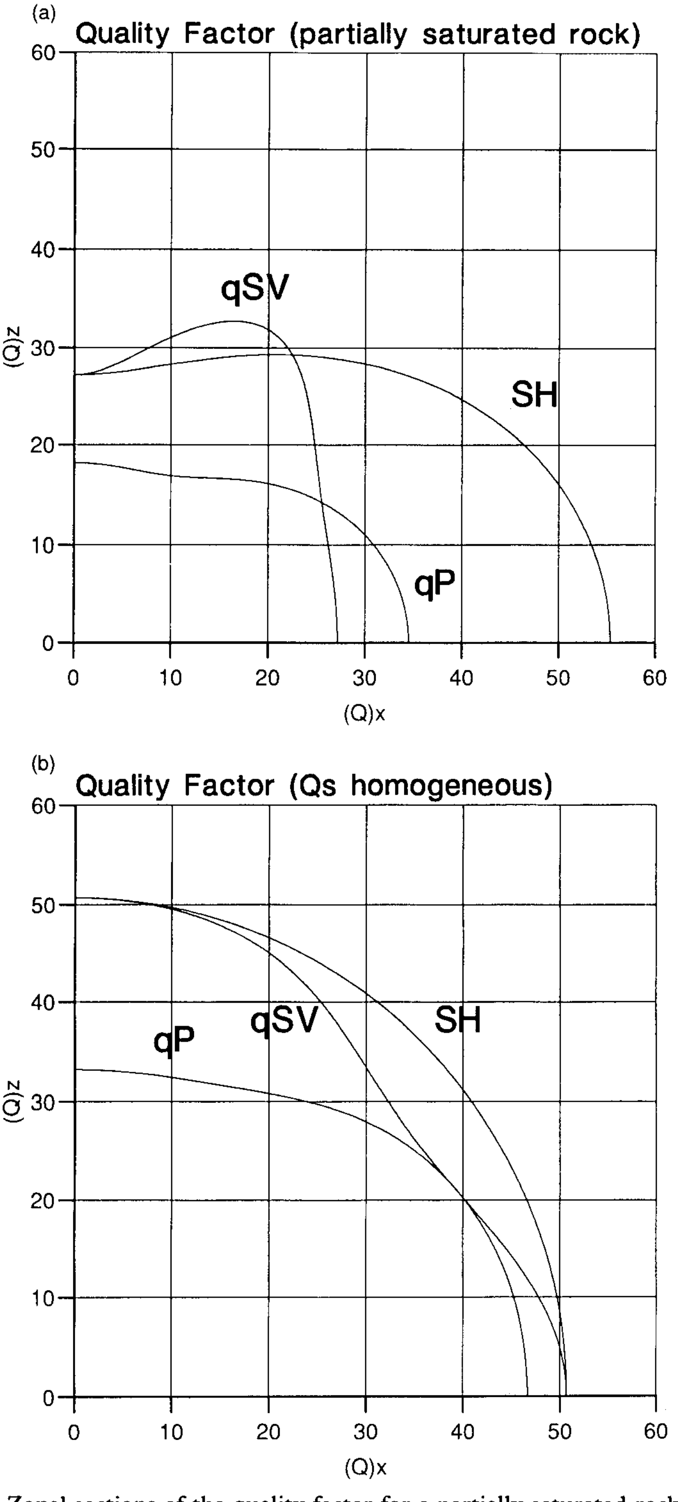

Figure 6. (a) Zonal sections of the quality factor for a partially saturated rock composed of ten constituents. Partial saturation implies that the bulk quality factors are smaller than the shear quality factors. (b) As Fig. 5, but $\bar{Q}_2 = 50$ for all the constituents.

Viscoelastic fluid-filled fractured systems

Backus theory can be used to describe a system of fluid-filled long and planar microfractures, provided that the size of the fluid boundary layer is greater than the thickness of the fracture. Moreover, if the fluid and the matrix rock are dissipative, the averaged system possesses an anisotropic intrinsic Q (Fig. 1b).

The shear complex modulus of a viscoelastic fluid can be modelled by a soft Kelvin–Voigt rheology. The term 'soft' means that the rigidity modulus is much less than the rigidities of typical rocks. This type of behaviour occurs when the fluid filling the cracks contains some kind of inclusion or colloidal suspension. The model can be represented by a spring of constant μ, and a dashpot of viscosity η parameterizing the Newtonian viscosity of the fluid (i.e. a Kelvin–Voigt model, see Ben-Menahem and Singh 1981). The behaviour of fluids in fractures of small size may depart from that of a Newtonian fluid (which is obtained when $\mu \to 0$) due to strong surface effects.

The complex modulus of the viscoelastic fluid is given by

$$\mu_{\mathrm{f}} = \mu + \mathrm{i}\omega\eta, \tag{10}$$

and the complex viscosity is defined by (e.g. Ferry 1970)

$$\eta^* = \frac{\mu_{\mathrm{f}}}{\mathrm{i}\omega} = \eta + \frac{\mu}{\mathrm{i}\omega}. \tag{11}$$

In contrast to ideal fluids, a real fluid with non-zero viscosity must satisfy a no-slip boundary condition. Near the solid–fluid interface, more precisely in the boundary layer, viscous waves of shear character propagate with complex wavenumber given by the frequency divided by the complex modulus (10), i.e.

$$k_{\mathrm{v}} = (1 - \mathrm{i})\sqrt{\frac{\omega\rho_{\mathrm{f}}}{2\eta^*}}, \tag{12}$$

where ρ_{f} is the fluid density. For a Newtonian fluid, $\eta^* = \eta$, and the wavelength of the viscous waves is

$$\lambda_{\mathrm{v}} = \frac{2\pi}{\mathrm{Re}\,(k_{\mathrm{v}})} = 2\pi\sqrt{\frac{2\eta}{\omega\rho_{\mathrm{f}}}}. \tag{13}$$

For oil at a pressure of 20 atm, the viscosity is $\eta = 445$ cp $= 0.445$ Kg/s/m, and the density is $\rho = 890$ Kg/m^3 (Winkler 1985). At the exploration seismic band, i.e. for a frequency of approximately 20 Hz, the viscous wavelength $\lambda_{\mathrm{v}} = 1.77$ cm, and for frequencies in the sonic band, say 2 KHz, the wavelength $\lambda_{\mathrm{v}} = 0.17$ cm. For brine, with $\eta = 1$ cp, and $\rho_{\mathrm{f}} = 1040$ Kg/m^3, the viscous wavelengths are 0.8 mm and 0.08 mm, respectively, for the exploration and sonic frequency bands.

The model of fluid-filled fractures assumes that the interfaces are bonded by imposing the condition that the viscous wavelength be greater than the thickness of the fractures. From Backus equations, the averaged medium is transversely isotropic, but actually it is a special class with only three independent stiffnesses since $c_{33} \approx c_{11}$ and $c_{12} \approx c_{13}$.

The following example examines a fractured limestone (see Table 1 for the limestone properties) where the volume ratio of the fractures is assumed to be 10^{-5}. The complex bulk modulus of the fluid is simply $\lambda_f = \lambda_f^e M_1$, and the shear modulus is given by (10). For oil and water, the elastic moduli are $\lambda^e = 1.94$ GPa and $\lambda^e = 1.96$ GPa, respectively, with a shear modulus modelled by one Kelvin–Voigt element of rigidity $\mu = 10^{-5}$ GPa. The values of the quality factors are $\bar{Q}_1 = 40$ and $\bar{Q}_2 = 20$ for the limestone, and $\bar{Q}_1 = 20$ for bulk dissipations of the fluid.

The wave characteristics of the oil-filled fractured system are shown in Fig. 7, where the wavefronts are highly anisotropic, in particularly the shear modes. The form of the quality factor curves changes substantially from 20 Hz to 10 KHz, governed by the characteristics of the fluid. This has a complex viscosity at low frequencies and behaves as a Newtonian fluid at high frequencies. While the

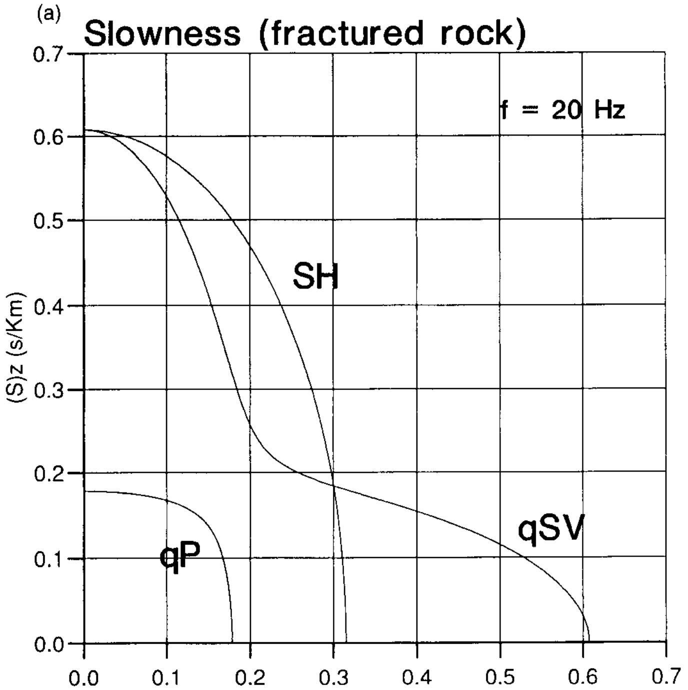

Figure 7. Zonal sections of the (a) slowness, (b) energy velocity, (c) and (d) quality factor surfaces and (e) attenuation for a fractured rock. The solid matrix is limestone and the fluid is oil whose complex viscosity (or complex rigidity modulus) is modelled by a 'soft'' Kelvin-Voigt rheology. The values of the quality factors are $\bar{Q}_1 = 40$ and $\bar{Q}_2 = 20$ for the limestone, and $\bar{Q}_1 = 20$ for bulk dissipations of the fluid.

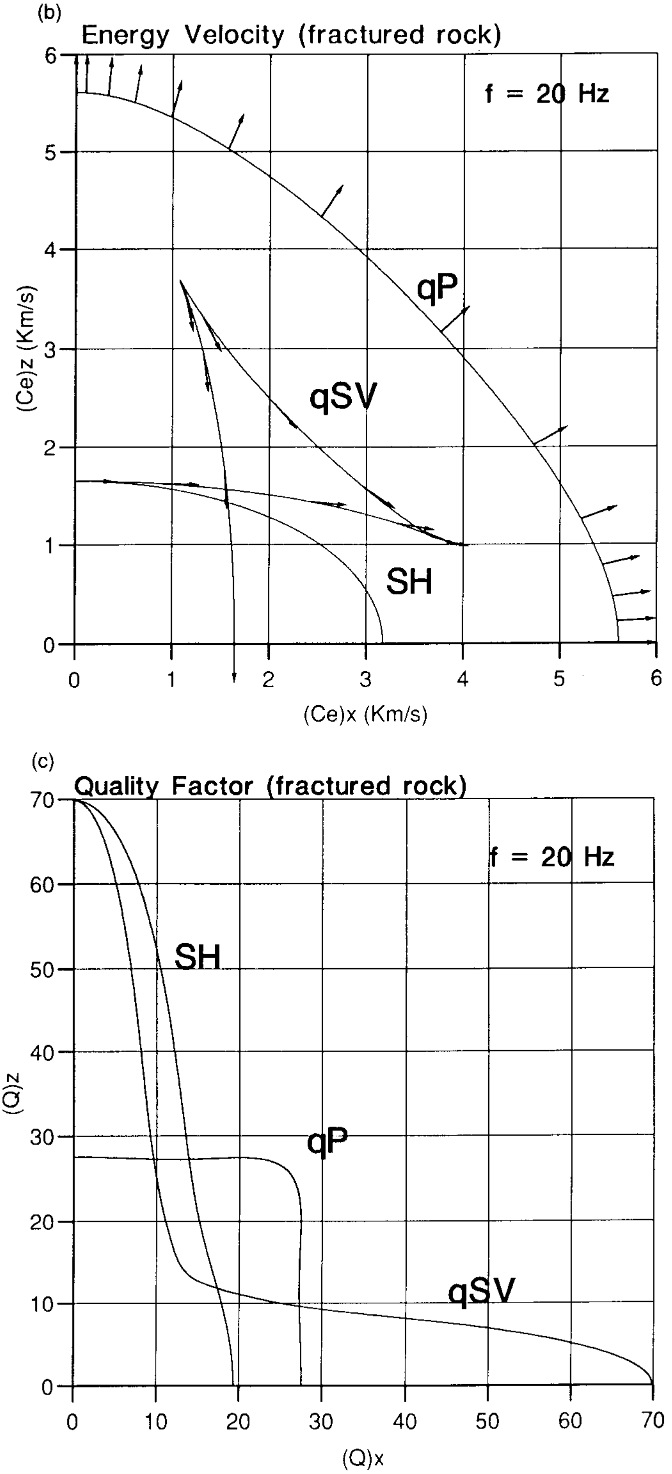

Figure 7. Continued

(d)

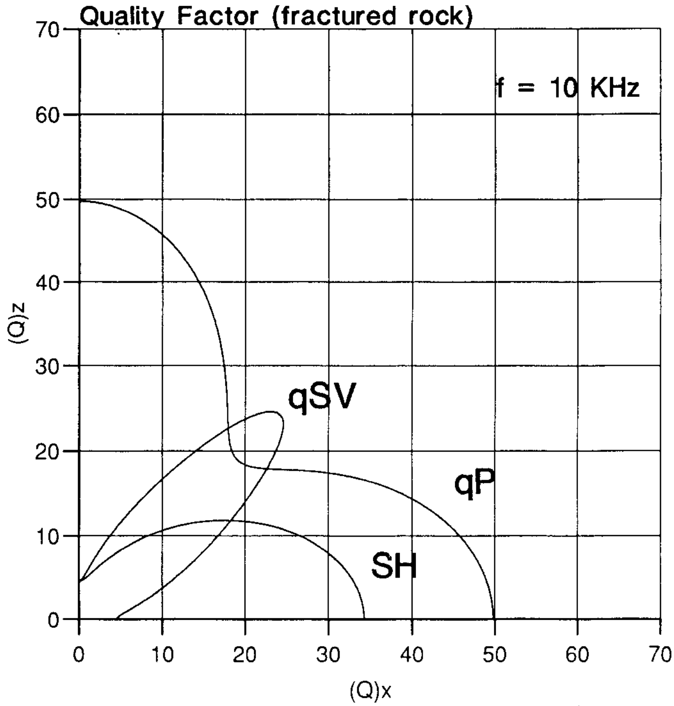
Quality Factor (fractured rock)
f = 10 KHz
qSV
qP
SH
(Q)z
(Q)x
0
10
20
30
40
50
60
70

(e)

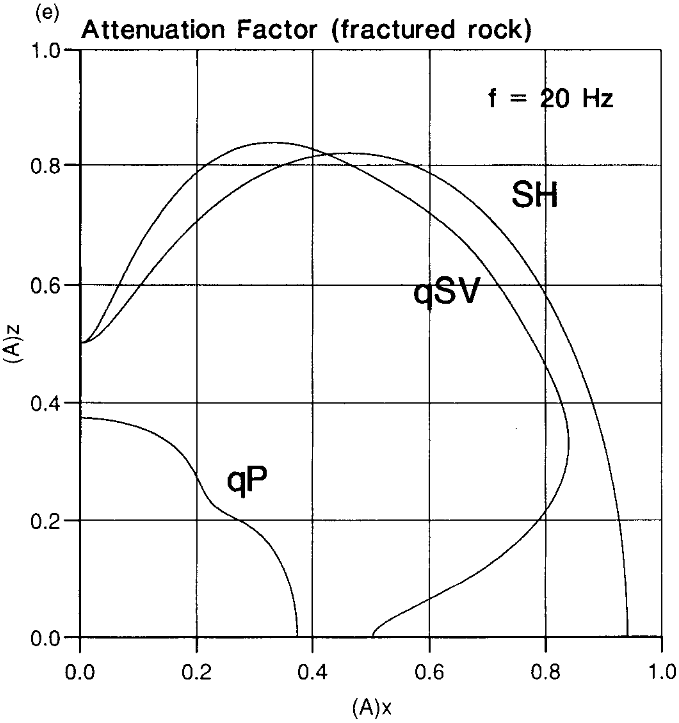
Attenuation Factor (fractured rock)
f = 20 Hz
SH
qSV
qP
(A)z
(A)x
0.0
0.2
0.4
0.6
0.8
1.0

coupled modes are symmetric with respect to the propagation direction at 45°, the pure SH mode is not, but follows the shape of the slowness curve. For a water-filled limestone, the quality factor is shown in Fig. 8; its characteristics are non-Newtonian at 10 KHz since the inertia term dominates the viscosity term in (11). In this case, the Newtonian behaviour is reached at higher frequencies.

Anisotropic and viscoelastic porous media

A model for layered porous media is obtained with alternating solid and fluid layers, the solid representing the matrix, and the fluid proportion, the porosity. In the long-wavelength limit, this model is a Biot anisotropic medium when the thickness of the fluid layers is large in comparison with the viscous wavelength (Fig. 1c). In this case, the fluid can be considered practically ideal, and perfect interfacial slip takes place. As a Biot solid, this system supports two compressional waves, the fast wave for which the solid and fluid displacements are in phase, and the slow wave with displacements 180° out of phase (Fig. 9) (For a complete review of Biot theory see Biot 1956; Bourbie, Coussy and Zinszner 1987). A Biot medium at very low frequencies does not support the slow wave since the viscosity effects dominate,

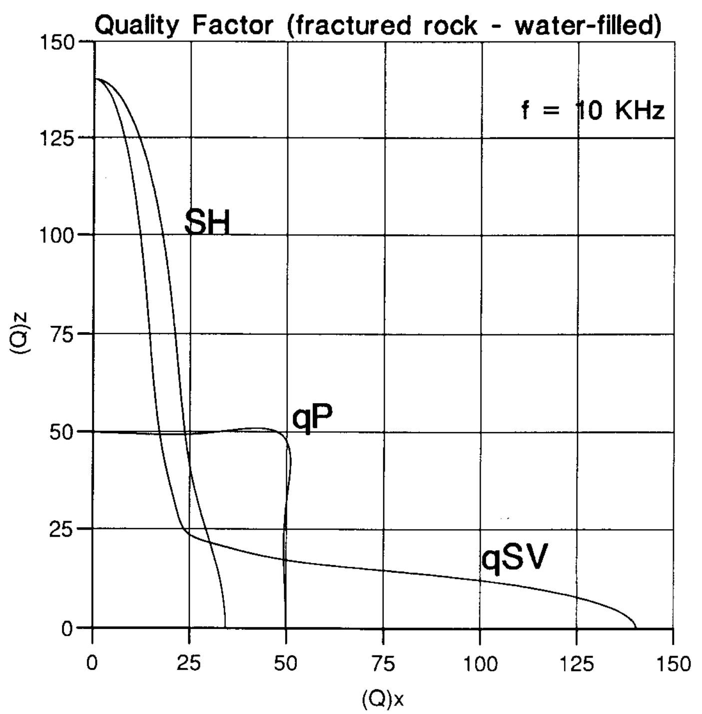

Figure 8. Quality factor for a water-filled fractured rock at 10 KHz. The only difference to Fig. 7 is the value of the fluid viscosity, which is much less for water than for oil.

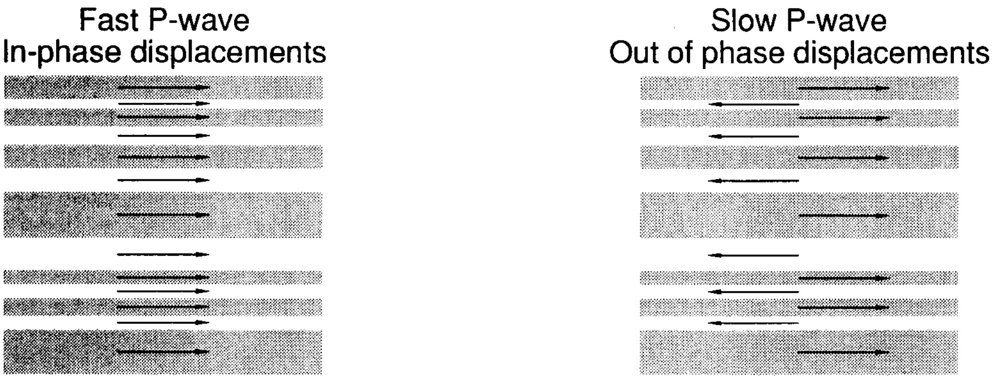

Figure 9. The anisotropic porous medium supports two compressional waves: the fast wave, for which the solid and fluid displacements are in phase, and the slow wave with displacements 180° out of phase.

and this mode becomes diffusive. When tangential slip takes place, the inertial effects are predominant and the Biot slow wave is activated. Here the effects due to viscoelasticity of the solid and fluid layers can be investigated for typical relative dimensions of grain (solid) and pore (fluid) sizes, a task that cannot be carried out within the framework of Biot theory. Shear-wave propagation is not of interest, since the layered porous medium propagates shear waves only along the direction of layering, with the velocity of the solid (Brekhovskikh 1980).

The dispersion equation for the elastic layered system was obtained by Schoenberg (1984). The viscoelastic system is obtained by substituting complex velocities for the elastic velocities. The dispersion equation is

$$V^4 + \left\{ -V^2 \left[\frac{l_z^2}{\langle \rho \rangle} + l_x^2 \left(\left\langle \frac{1}{\rho} \right\rangle + \frac{\phi V_{\mathrm{pl}}^2}{\rho_{\mathrm{f}} V_{\mathrm{f}}^2} \right) \right] + V_{\mathrm{pl}}^2 l_x^2 \left(\frac{\phi l_x^2}{\rho_{\mathrm{f}}} + \frac{l_z^2}{\langle \rho \rangle} \right) \right\} \left\langle \frac{1}{\rho V_{\mathrm{P}}^2} \right\rangle^{-1} = 0, \quad (14)$$

where V_{P} refers to compressional velocity, denoted by V_{f} for the fluid, ϕ is the porosity, ρ_{f} is the density of the fluid, and $V_{\mathrm{pl}} = 2(1 - V_{\mathrm{S}}^2/V_{\mathrm{P}}^2)^{1/2} V_{\mathrm{S}}$ is the long wavelength complex velocity of extensional waves in an infinite plate, with V_{S} and V_{P} the shear and compressional complex velocities of the solid, respectively. The bracket operation $\langle \cdot \rangle$ denotes thickness weighted average.

Equation (14) has two physical solutions, corresponding to the fast and slow compressional waves. The medium is anisotropic since the density is a transversely isotropic tensor with effective density $\langle \rho \rangle$ normal to the layering, and effective density $\langle 1/\rho \rangle^{-1}$ parallel to the layering.

The phase velocity is the frequency divided by the real wavenumber. As in the bonded interface case (Carcione 1992), its magnitude is given by

$$c_{\mathrm{p}} = \left[\mathrm{Re} \left(\frac{1}{V} \right) \right]^{-1}. \quad (15)$$

Similarly, the magnitude of the attenuation vector is given by

$$\alpha = -\omega \, \mathrm{Im}\left(\frac{1}{V}\right). \tag{16}$$

An energy analysis is beyond the scope of this work. Thus, a precise formula for the wave surface as given by the energy velocity will not be developed. Similarly, it is not clear whether the expression for the quality factor obtained from the Backus model (Carcione 1992) applies to this case. Attenuation and wave surfaces are described by the absorption coefficient and the group velocity, the latter representing an approximation of the wavefront surface for anelastic media. The formula for the group velocity surface is obtained in Appendix B.

The following example considers a limestone matrix filled with water. The attenuation characteristics of the constituents are the same as for the fractured limestone with the difference that here the rigidity modulus of the fluid is negligible, and therefore the viscous skin is much smaller than the size of the pores. Figure 10 shows the wave characteristics of the porous medium for two different values of the porosity, (a) $\phi = 0.1$, and (b) $\phi = 0.5$, at a frequency of 10 Khz. As can be seen from the phase and group velocity curves, the slow wave does not propagate in the neighbourhood of the vertical direction since the solid and fluid displacements are in phase in that region. The waves are highly anisotropic with faster velocities along the directions of the pores. In particular the slow waves presents pronounced cusps. Higher porosity implies significant reduction of the fast wave velocity only in the vertical direction. Unlike the fractured model, the attenuation curves do not change significantly with frequency in the range where the quality factors of the constitutents are constant. Here the effects of the fluid viscosity are not important, since the model does not consider the Biot mechanism. For a given porosity, the slow wave is more attenuated than the fast wave and, for increasing porosity, the attenuation along the vertical direction increases relatively more than in the horizontal direction. The fact that the slow wave does not propagate in the neighbourhood of the vertical direction is also evident in the attenuation curves, where it is indicated by the infinite value of the attenuation factor.

Conclusions

This work investigates the anisotropic characteristics of wave propagation in reservoir environments by means of three simplified models based on plane-layered structures, where particular attention is given to the attenuation properties. Fine layering shows a variety of behaviours depending on the intrinsic attenuation that is used to model total and partial saturation of the single constituents. The quality factor surfaces of the three propagating modes indicate that the qSV mode is the most affected by a transition from total to partial saturation. In general, the dissipation is higher along the symmetry axis direction when the quality factors are

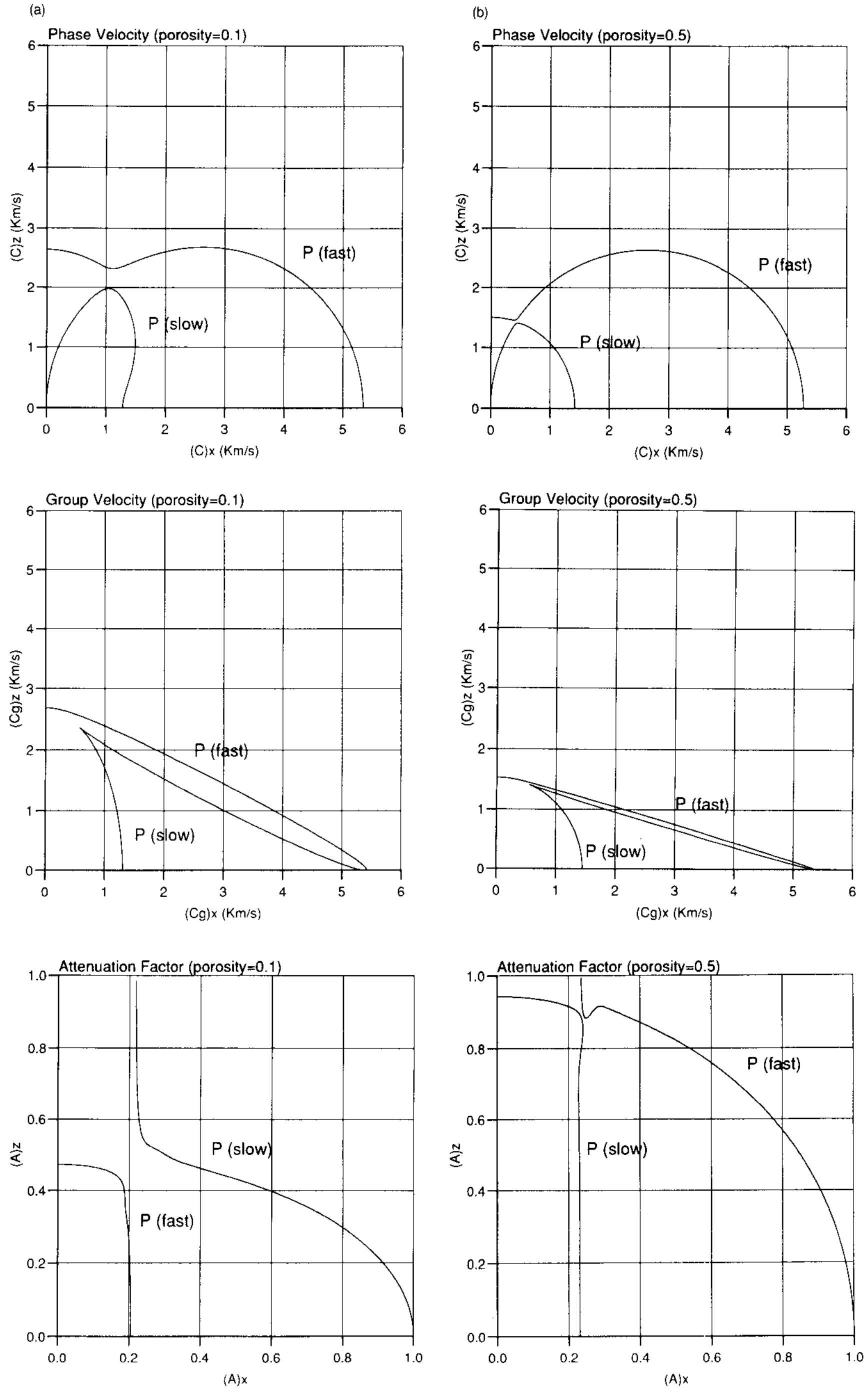

Figure 10. Zonal sections of the phase velocity, group velocity and attenuation factor in a layered porous medium for two different porosities, (a) $\phi = 0.1$ and (b) $\phi = 0.5$. Frequency is 10 KHz. The medium is limestone filled with water, and the attenuation characteristics of the constituents are the same as for the fractured limestone of Fig. 7.

proportional to the wave velocities, and vice versa when inversely proportional to the velocity. On the other hand, the energy velocity surfaces are not substantially affected by the intrinsic dissipation. This implies that the attenuation surfaces can be better indicators of the direction of layering, and its degree of saturation, than the respective wavefronts.

Similarly, the attenuation in fluid-filled fractured rocks, where the fluid is explicitly modelled by a thin layer, strongly depends on the frequency range and the fluid viscosity. When viscosity effects dominate (i.e. at high frequencies), the shear waves are highly attenuated perpendicular to the fracture strike. When the inertial term is predominant (i.e. at low frequencies), the qP wave presents, in general, the highest dissipation along all the propagation directions.

Layered porous media describe the wave behaviour on a local scale assuming that the pores are of planar shape. In this context, the wavefront and attenuation are very anisotropic, the anisotropy increasing with increasing porosity. The propagation of the slow wave is forbidden along the direction perpendicular to the layering, and its wavefront resembles a cuspidal triangle similar to the cusp of a qSV wave in a single-phase anisotropic medium. The implementation of these rheologies into modelling codes should give support to the theory and more insight into the physical processes involved.

Acknowledgements

This work was funded in part by the European Commission in the framework of the JOULE programme, sub-programme Advanced Fuel Technologies. I thank Julie Hood and Joe Dellinger for very detailed reviews of the article.

Appendix A

Polarizations in anisotropic-viscoelastic media

Polarization of the different wave modes in the (x, z)-plane can be calculated from the Christoffel equation (9). The SH mode is polarized only along the y-direction, while the coupled modes have components exclusively in the (x, z)-plane. The first line of (9) yields

$$(c_{11} l_x^2 + c_{55} l_z^2 - \rho V^2) u_x + (c_{13} + c_{55}) l_x l_z u_z = 0. \tag{A1}$$

It is clear that the complex vector $[1, 0, u_z/u_x]^{\mathrm{T}}$ is also an eigenvector of the Christoffel equation (9). Then, the normalized polarizations vectors of the coupled modes are

$$\{1 + [\mathrm{Re}\,(B_m)]^2\}^{-1/2} [1, 0, \mathrm{Re}\,(B_m)]^{\mathrm{T}}, \qquad m = 1, 2, \tag{A2}$$

where

$$B_m = -\frac{c_{11}l_x^2 + c_{55}l_z^2 - \rho V_m^2}{(c_{13} + c_{55})l_x l_z}, \tag{A3}$$

and where $m = 1$ and $m = 2$ correspond to the qP and qSV waves, respectively. The SH polarization vector is perpendicular to the (x, z)-plane.

The deviation of the viscoelastic polarization from the elastic polarization can be quantified by computing the difference between the polarization angles with respect to the x-axis.

$$\Delta\gamma(\omega, \theta) = \arctan\left[\mathrm{Re}\,(B_1(\omega, \theta))\right] - \arctan\left[B_1(0, \theta)\right], \tag{A4}$$

where $\theta = \arccos(l_z)$.

Appendix B

Group velocity for alternating solid and fluid layers

The group velocity is the velocity of the modulation envelope of the wave and, as in the elastic case, can be expressed by

$$\mathbf{c}_g = \hat{\mathbf{e}}_x \frac{\partial\omega}{\partial\kappa_x} + \hat{\mathbf{e}}_y \frac{\partial\omega}{\partial\kappa_y} + \hat{\mathbf{e}}_z \frac{\partial\omega}{\partial\kappa_z}, \tag{B1}$$

where the spatial derivatives are taken with respect to the real wavenumber. Since a real explicit relationship of the form $\omega = \Omega^R(\kappa_x, \kappa_y, \kappa_z)$ is not available, (B1) is not appropriate. Alternatively, the group velocity can be obtained by implicit differentiation of the dispersion relation (14). For instance, for the x-component,

$$\frac{\partial\omega}{\partial\kappa_x} = \left(\frac{\partial\kappa_x}{\partial\omega}\right)^{-1}, \tag{B2}$$

or, since $\kappa_x = \mathrm{Re}\,(k_x)$,

$$\frac{\partial\omega}{\partial\kappa_x} = \left[\mathrm{Re}\left(\frac{\partial k_x}{\partial\omega}\right)\right]^{-1}. \tag{B3}$$

Implicit differentiation of the complex dispersion relation $\Omega(k_x, k_y, k_z, \omega) = 0$ gives

$$\left(\frac{\partial\Omega}{\partial\omega}\delta\omega + \frac{\partial\Omega}{\partial k_x}\delta k_x\right)_{k_y, k_z} = 0. \tag{B4}$$

Thus,

$$\left(\frac{\partial k_x}{\partial\omega}\right)_{k_y, k_z} = -\frac{\partial\Omega/\partial\omega}{\partial\Omega/\partial k_x}, \tag{B5}$$

and similar relations hold for the k_y and k_z components. Replacing the partial derivatives in (B1), the group velocity can be evaluated as

$$\mathbf{c}_g = -\left\{\hat{\mathbf{e}}_x \left[\mathrm{Re}\left(\frac{\partial\Omega/\partial\omega}{\partial\Omega/\partial k_x}\right)\right]^{-1} + \hat{\mathbf{e}}_y \left[\mathrm{Re}\left(\frac{\partial\Omega/\partial\omega}{\partial\Omega/\partial k_y}\right)\right]^{-1} + \hat{\mathbf{e}}_z \left[\mathrm{Re}\left(\frac{\partial\Omega/\partial\omega}{\partial\Omega/\partial k_z}\right)\right]^{-1}\right\}. \tag{B6}$$

For the alternating solid–fluid layered system, the complex dispersion relationship is obtained from (14) and the expression for the complex wavevector is

$$\mathbf{k} = \frac{\omega}{V}\,(l_x \hat{\mathbf{e}}_x + l_z \hat{\mathbf{e}}_z). \tag{B7}$$

Thus,

$$\Omega(k_x, k_z, \omega) = V_{\mathrm{pl}}^2 k_x^2 \left(\frac{\phi k_x^2}{\rho_{\mathrm{f}}} + \frac{k_z^2}{\langle\rho\rangle}\right) - \omega^2\left[\frac{k_z^2}{\langle\rho\rangle} + k_x^2\left(\left\langle\frac{1}{\rho}\right\rangle + \frac{\phi V_{\mathrm{pl}}^2}{\rho_{\mathrm{f}} V_{\mathrm{f}}^2}\right)\right] + \omega^4\left\langle\frac{1}{\rho V_{\mathrm{P}}^2}\right\rangle = 0. \tag{B8}$$

The evaluation of the group velocity from (B6) is performed first through explicit calculation of the partial derivatives, and then by numerical evaluation of the final formula. The calculation of the partial derivatives with respect to the wavenumber components is straightforward, while $\partial\Omega/\partial\omega$ requires more effort because each complex velocity in (B8) is frequency-dependent. Since only squared velocities appear in the formula, the last step of the calculation includes the explicit derivatives of the dimensionless moduli (2), which are

$$\frac{\partial M_\nu}{\partial\omega} = \left(\frac{2}{\pi \bar{Q}_\nu}\right)\frac{\mathrm{i}(\tau_1 - \tau_2)M_\nu^2}{(1 + \mathrm{i}\omega\tau_1)(1 + \mathrm{i}\omega\tau_2)}, \qquad \nu = 1, 2. \tag{B9}$$

References

Auld B.A. 1990. *Acoustic Fields and Waves in Solids, Vol. 1*, 2nd edn. Robert E. Krieger Publ. Co.

Backus G.E. 1962. Long-wave elastic anisotropy produced by horizontal layering. *Journal of Geophysical Research* 67, 4427–4440.

Ben-Menahem A.B. and Singh S.J. 1981. *Seismic Waves and Sources.* Springer Verlag, Inc.

Biot M.A. 1956. Theory of propagation of elastic waves in a fluid-saturated porous solid. I. Low-frequency range. *Journal of the Acoustical Society of America* 28, 168–178.

Bourbie T., Coussy O. and Zinszner B. 1987. *Acoustics of Porous Media.* Institut Francais du Petrole Publications.

Brekhovskikh L.M. 1980. *Waves in Layered Media*, 2nd edn. Academic Press, Inc.

Carcione J.M. 1992. Anisotropic Q and velocity dispersion of finely layered media. *Geophysical Prospecting* **40**, 761–783.

Carcione J.M. 1994. Wavefronts in dissipative anisotropic media. *Geophysics* **59**, 644–657.
Carcione J.M., Kosloff D. and Behle A. 1991. Long-wave anisotropy in stratified media: A numerical test. *Geophysics* **56**, 245–254.
Ferry J.D. 1970. *Viscoelastic Properties of Polymers*. John Wiley & Sons, Inc.
Postma G.W. 1955. Wave propagation in a stratified medium. *Geophysics* **20**, 780–806.
Schoenberg M. 1984. Wave propagation in alternating solid and fluid layers. *Wave Motion* **6**, 303–320.
Schoenberg M. and Douma J. 1988. Elastic wave propagation in media with parallel fractures and aligned cracks. *Geophysical Prospecting* **36**, 571–590.
Winkler K.W. 1985. Dispersion analysis in Berea sandstone. *Journal of Geophysical Research* **89**, 11549–11559.